Particuology 93 (2024) 364–376

Contents lists available at ScienceDirect

Particuology

journal homepage: www.elsevier.com/locate/partic

Coating powder beds with liquids and foams based on viscous formulations using a twin screw mixer: A continuous process study

Mohamed S. Manga [a, 1, **], Dimitrios Kontziampasis [a, b, c, d, 1, *], Mustafa Al-Maqdad [a], Sean Clifford [e, f], Serafim Bakalis [f, g], David W. York [a]

[a] School of Chemical and Process Engineering, Faculty of Engineering and Physical Sciences, University of Leeds, Leeds, LS2 9JT, UK
[b] School of Mechanical Engineering, Faculty of Engineering and Physical Sciences, University of Leeds, Leeds, LS2 9JT, UK
[c] School of Science and Engineering, University of Dundee, DD1 4HN, Dundee, Scotland, UK
[d] Dundee International Institute of Central South University, Tongzipo Road, Central South University, Changsha, Hunan, 410013, China
[e] Department of Chemical Engineering, School of Engineering, University of Newcastle, Newcastle, NE1 7RU, UK
[f] School of Chemical Engineering, University of Birmingham, Birmingham, B15 2TT, UK
[g] Department of Chemical Engineering, Faculty of Engineering, University of Nottingham, NG7 2RD, UK

A R T I C L E I N F O

Article history:
Received 19 March 2024
Received in revised form
15 July 2024
Accepted 18 July 2024
Available online 31 July 2024

Keywords:
Powder coating
Continuous processing
Viscous liquid
Foam
Image analysis
Positron emission particle traking (PEPT)

A B S T R A C T

Coating with viscous formulations has been essential in numerous industries as it can be a means for providing functionalization, additional properties, as well as other benefits. However, there have been scarce studies that have investigated and proposed methodologies in literature. Continuous coating of powders with viscous liquids poses as a promising technology, which has been mentioned in some studies, but has not yet been thoroughly investigated. This paper employs the use of image processing and analysis, in combination with statistical analysis of particles to evaluate the effectiveness of foams and liquids as a means of coating powder beds. Two different sizes of twin screw mixers that are working in continuous operation are employed, and a new continuous foaming device is fabricated and used for the experiments of coating. The effect of materials and process parameters (as for example rotational speed, and flowrate) on the quality of coating are investigated. Image analysis is used to assess the coating quality. The results clearly showcase the potential of using twin screw mixers for coating purposes and not only for mixing. The hypothesis that using large bubble foams to improve the coating of viscous liquids on particles is proven correct, as they provide higher quality coatings compared to their equivalent liquids, when used in the twin screw mixer. Surprisingly, using a larger scale twin screw mixer, does not show a substantial effect on the mixing, regarding quality, however there is still a requirement for mix optimization for achieving scale-up of this process. These results provide a new pathway for coating powders with viscous formulations in industrial applications, requiring less energy and effort in this process, and can pave the way towards introducing more sustainable industrial methodologies for coating.

1. Introduction

Coating powder products with a thin film of liquid is an important processing step in numerous applications, especially within the pharmaceutical, food, personal-care, and agrochemical industries (Salman et al., 2007). These coatings are normally applied in order to improve the physico-chemical properties of the powder, i.e. colour and aesthetics, storage stability, taste-masking, ability for triggered and controlled release, as well as to modify the powder flowability and its density (Cole, 1995, pp. 1–5; Fuchs et al., 2006; Nedovic et al., 2011; Onwulata, 2005). In many of

* Corresponding author. Mechanical Engineering, School of Science and Engineering, University of Dundee, DD1 4HN, Dundee, UK.
** Corresponding author. School of Chemical and Process Engineering, Faculty of Engineering and Physical Sciences, University of Leeds, Leeds, LS2 9JT, UK.
E-mail addresses: mohamedsmanga@gmail.com (M.S. Manga), dkontziampasis001@dundee.ac.uk, d.kontziampasis@gmail.com (D. Kontziampasis).
[1] These authors contributed equally to this work.

https://doi.org/10.1016/j.partic.2024.07.012
1674-2001/

these applications, the distribution of the coating material within the powder bed is critical for the intended performance, whilst the ability to control the coating coverage on every particle (i.e. % of particle covered with the coating liquid) is less critical, but often a desirable feature.

Coating powders with a liquid film is traditionally done using fluidised bed, panning and dipping techniques. The choice of process is dependent on the properties of the powder and the coating material. The most extensively used technique is fluidised bed coating and in particular the Wurster process (Wurster, 1959), where the coating material is usually sprayed into the moving bed, often as a dilute solution. Although the quality of the powder coating (particle to particle coating uniformity and control of film porosity) is high, there are some drawbacks in the use of this method. The resulting product suffers from long processing times, whilst the overall product throughput is usually low, mainly due to typically operating in batch mode, requiring increased drying times and typically resulting is higher cost (Plank et al., 2003). Fluidised beds are often expensive capital items and require additional separation systems to remove the fluidising air. Low viscosity fluids are preferred as they can be easily sprayed, whereas nozzle blockages and pumping issues are often associated with spraying of high viscosity fluids. This reduces flexibility in the choice of coating materials that can be used.

Paddle mixers offer an alternative approach to these traditional coating techniques. The paddles are orientated to impart lateral and/or axial mixing (Paul et al., 2004), and can be operated both in batch and continuous modes (with cycle times of 10 s to a few minutes). The twin shaft paddle mixer (often referred to as a twin screw mixer (TSM)) is based on a screw conveyor (auger) design that not only conveys the material, but also eliminates potential dead spaces during the mixing process within the vessel, via overlapping the screw paths. In a counter-rotating TSM, the particles are lifted upwards starting from the bottom of the trough to the middle of the mixer vessel (known as the fluidised zone). This is where the mixing process takes place, in a weightless state due to the centrifugal force generated by the paddles (Equipment). The advantages of using this type of a mixer are the following; i) they are self-cleaning due to the high tip speeds that can be achieved (Ennis, 2010), ii) they provide flexibility in paddle and mixer designs in order to influence residence time distributions, iii) they are able to achieve high throughputs, and iv) a plethora of powders and coating materials with a wide spectrum of properties can be used.

The fundamental processes that are involved in coating individual powder particles with liquids, are similar to those that are in wet granulation. Wet granulation is the process used for particle size enlargement, and its processes are widely documented in a variety of regime maps (Hapgood et al., 2003; Iveson et al., 2001; Iveson & Litster, 1998; Rough et al., 2005). Recent wet granulation studies investigating aqueous foam binders, have found that the properties of the granules were similar to those created via conventional liquid sprays (Cantor et al., 2009; Keary & Sheskey, 2004; Sheskey et al., 2007). Furthermore, foam binders provide numerous advantages over liquid binders, such as improved binder dispersion, wetting throughout the powder, need for less binder, and simpler addition methods as there is no need for using nozzles (Tan et al., 2009; Tan & Hapgood, 2011a, 2011b). Foams have also been used as an alternative coating method for numerous applications (Gregorian et al., 1979; Kenttä et al., 2014; Kinnunen-Raudaskosko et al., 2014; Sievänen, 2010; Thompson, Weatherley, et al., 2012).

To the best of our knowledge, studies investigating the incorporation of foams into moving powder beds operating in a continuous mode have been explored by Thompson et al. and are tailored towards wet granulation using twin screw granulators (operates differently to the twin screw mixer) (Li, Thompson, & O'Donnell, 2015; Li, Thompson, & O'Donnell, 2015; Rocca et al., 2015; Thompson, 2015; Thompson, Mu, & Sheskey, 2012; Thompson and O Donnell, 2015; Weatherley et al., 2013). The present work builds on our previous work on batch operation and expands it (Kontziampasis et al., 2020). Herein, initially the ability to convert model coating liquids of different viscosities into foams is explored in a continuous manner, using a sparger setup. Subsequently, an investigation is showcased for the first time in literature on how these continuously generated foams can be used to coat a moving powder bed within a TSM, operating in continuous mode. With the aid of image analysis, the performance of the continuous foam coating process is evaluated against the traditional spray on method. Finally, the entire process is explored in terms of its impact when the TSM is scaled up, as well as on the use of technologies as for example Positron Emission Particle Tracking that pose as indispensable for the understanding of the mixer characteristics.

2. Materials and methodology

2.1. Materials

Granular Sodium Sulphate (Grupo Crimedesa, Spain) with a mean particle size of 150–250 μm was used as a model powder system. Granulated sugar (Tate & Lyle) was purchased from a local supermarket (Leeds). Whey protein concentrate (unflavoured Whey protein 80) was purchased from The Protein Works. Liquitint® Red ST dye (Milliken Chemical) was used in order to visualise the distribution of the liquid/foam used to coat the powders. Distilled water was used in the preparation of all solutions.

2.2. Methodology

Preparation of sugar-protein solutions: Liquid viscosity was controlled by changing the ratio of added sugar to distilled water. The composition and viscosities of the liquids used in these study have been previously detailed in our earlier publication (Kontziampasis et al., 2020). Briefly, 400 g of water was heated in a beaker to 80 °C using a magnetic hot-plate stirrer. Subsequently, the required amount of sugar was added slowly and allowed to mix using a magnetic stirrer until the sugar fully dissolved. This sugar solution was left to cool down to room temperature before adding it to a 1.5 L Kenwood blender (FDM781BA model). 80 g of whey protein powder and 2 mL of Liquitint® Red ST dye was added to the mixture, and blended at the maximum blender speed for 20 min. The resulting sugar-protein solution was allowed to rest after mixing to remove any entrained air.

Preparation of foam: For large bubble sized foams, the sugar-protein solutions were pumped (using a Watson Marlow peristaltic pump) into the base of a custom-built foaming rig. This consists of a Perspex® column equipped with a 20 μm porous ceramic sparger (Fairey Technical Ceramics, U.K.) (located above the liquid inlet point (Fig. 1(a))). The column has an internal diameter of 10 cm and a height of 1.5 m. Once the liquid level reaches above the height of the sparger, the compressed air line to the sparger is turned on in order to produce the required foam. The column was fixed at an angle of 15° to the TSM so that once the column filled up with foam it could exit directly into the TSM via a top inlet port (Fig. 1(b)). An overall schematic of how the foaming column, the TSM mixer and the conveyor belt for imaging are setup is illustrated in Fig. 1(c). It is important to note that the foam that is used in this work has been introduced in the previous work (Kontziampasis et al., 2020) of the group, including the reasoning behind the use of the specific composition. By default the formulation follows the same composition as Formulation 2 in (Kontziampasis et al., 2020), unless it is stated otherwise.

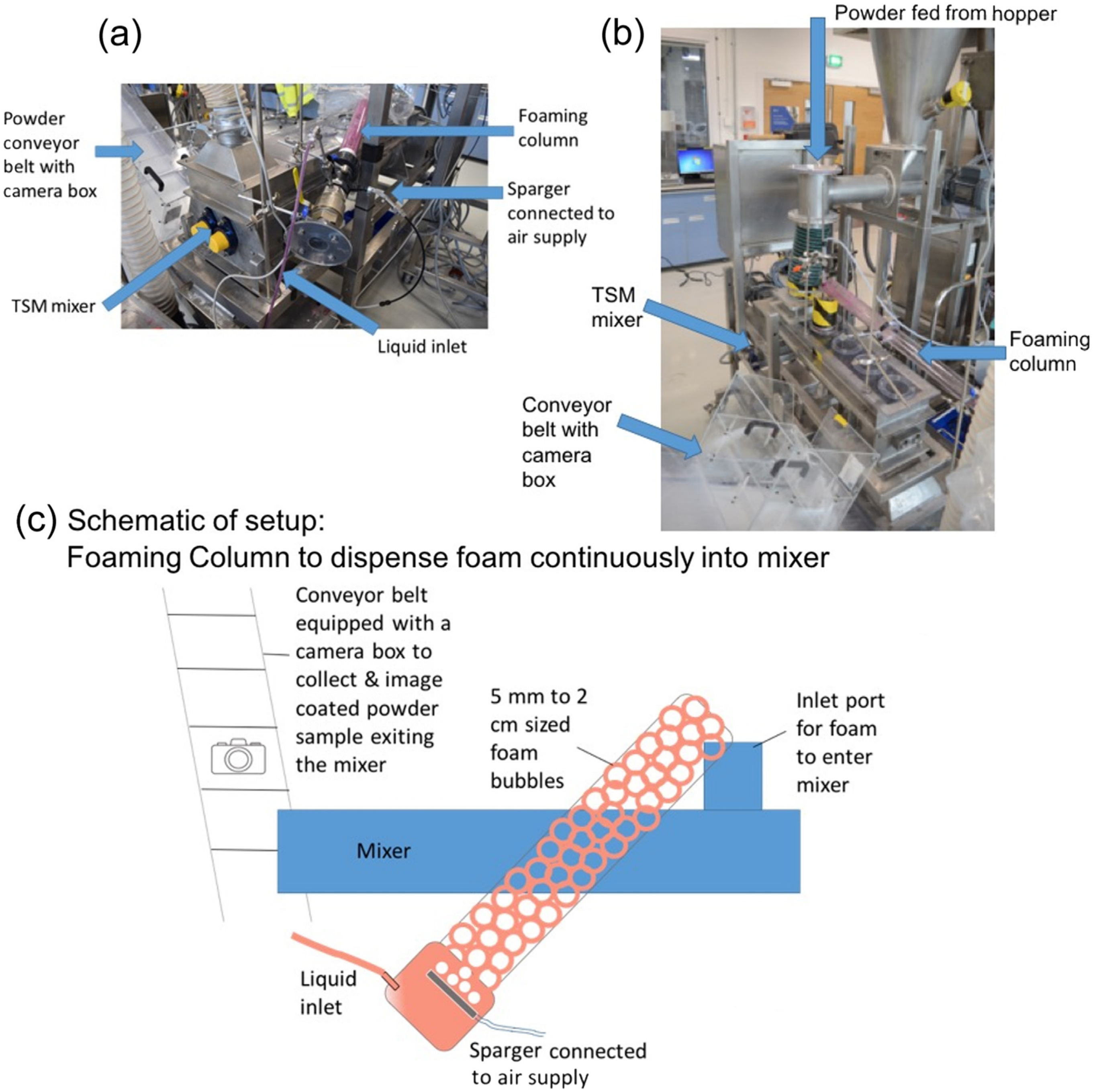

Fig. 1. Illustration of (a) liquid inlet feed and sparger position within the base plate of custom-built perspex foam column additionally shown in the schematic and (b) set-up of the perspex foam column to allow addition of foam to the powder via a top inlet port for continuous operation. (c) Schematic representation of the process, as can be seen in (a) and (b), showing the overall layout of the setup. The powder subsequently goes onto conveyor belt to allow imaging of the product for colour analysis.

Continuous liquid/foam coating of powders: In this study, a TSM 75 (Ajax Equipment Ltd, U.K.) was set up in continuous mode in a way that all the powder was conveyed in a forward conveying motion by adjusting the quadrant paddles on the shafts to 20°. The number 75 corresponds to the mixing element diameter, and is expressed in mm. The powder was fed using a hopper equipped with a screw auger (Feeder 100, Ajax Equipment Ltd, U.K.) to control the powder fill level inside the TSM. The feeder motor was operated at either 5 or 9 Hz, corresponding to powder throughput of 196 and 405 kg/h. The speed range of the motor driving the twin shafts of the TSM was investigated from 15 to 70 Hz. Typically, the TSM was turned on at the desired motor speed after which the hopper was turned on to feed the TSM and achieve the desired fill level. The mixer was allowed to run for a few minutes with the dry base powder in order to reach equilibrium (steady state). After reaching equilibrium, the liquid (added by directly pumping via a tube into the TSM) or the foam (using the custom-built foaming rig, Fig. 1) was introduced continuously into the mixer via a top inlet port. In our previous publication (Kontziampasis et al., 2020) we prepared the foams using a batch operation via two different methods. The first method was placing the viscous liquid in a beaker and then using the sparger to make a beaker full of foam.

This foam was classed as large bubble foam. The second method was placing the viscous liquid into a food blender and then mixing it at high shear to obtain a jug of foam which we classified as small bubble foam. To determine the effect of scaling up the process, a larger TSM was also used (TSM 125, i.e. 125 mm mixing element diameter). Considerations for the scale up study was i) keeping the powder turnover rate by operating at similar motor speeds, ii) achieving similar powder fill level in the TSM by increasing the powder fill rate to achieve comparative powder mixing between the two TSM sizes.

Image analysis of coated products: The product that exited the TSM mixer was placed onto a conveyor belt equipped with an enclosure to video the moving powder using an Nikon D3200 DSLR camera operating at 60 frames per second. A video of around 3–5 min was recorded on each run, which was then used to obtain frames (invidual images) for further analysis. These images were analysed using a custom-made software developed within MATLAB®, which plots the colour distribution based on either red, blue, or green colour components. For this study, the red colour component was chosen for analysis due to the use of a red dye. Calibrations were done to determine the red colour distribution within the red dye as well as within the white powder used. This is the percentage of the red colour component within the combined RGB colour space. For example, a sample that has an equal amount of the red, blue and green colour components would register a mean value of 33.33% for each component. For analysis of the coated product at each test condition studied, at least 3 different powder samples were subjected to image analysis and the typical error encountered during processing was within 2%–5% in each case that was studied.

Benchmark studies: The red colour distribution within the powder and the Liquitint® Red dye were processed using image analysis (Fig. 2). Since the uncoated sodium sulphate powder is white it will contain a combination of the three individual colour components of red, green and blue. The red colour distribution within the white powder is narrow with a sharp peak (indicating homogeneity) as expected, with a mean % red value of 36 (i.e. just over a third red compared to its blue and green counterparts. The maximum peak intensity value obtained here matches well with that observed in the previous study (~1.8) (Kontziampasis et al., 2020). The dye in contrast has a greater % of red within the image (as is expected) but the distribution is very broad (38%–48%) with a low maximum peak intensity value of 0.5. These two distributions provide the absolute limits in which the coated samples will fall within.

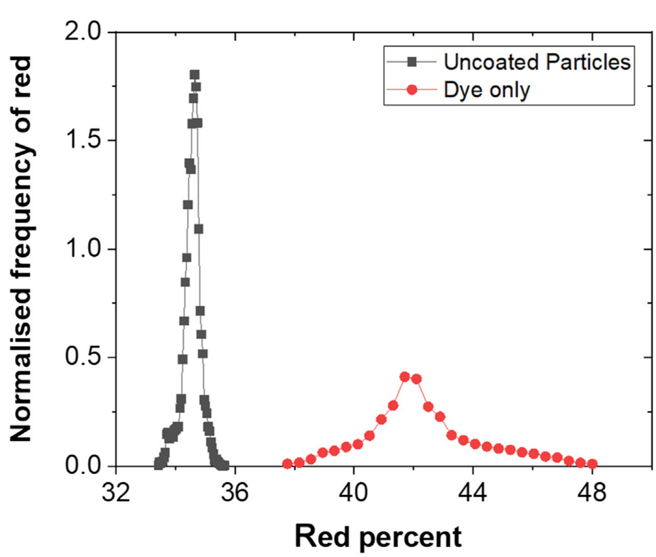

Fig. 2. Normalised histograms of red colour component (i.e. (red/green + blue)*100) in the uncoated white sodium sulphate particles and dye used for this study. (For interpretation of the references to colour in this figure legend, the reader is referred to the Web version of this article.)

To determine a performance baseline of the TSM mixer running continuously, the low viscosity dye solution was sprayed onto a fluidised sodium sulphate powder bed using a two fluid nozzle. For this study a powder feed rate of 196 kg/h and a TSM motor speed of 30 Hz was used. By splitting the video into a series of images, a snapshot of the powder coating process can be visualised with respect to time (Fig. 3(a)). It is envisaged that the coating process occurs as follows; 1) powder enters into the mixer from the feeder and is agitated by the paddles and conveyed forwards towards the spray zone, 2) fine droplets of the dye solution are sprayed on onto a proportion of the powder as it enters the spray zone, and 3) the fluidisation of these wetted particles cause them to interact with non-wetted particles that shears the liquid around the particle similar to that seen in fluidised bed coating processes. In addition, during this contact time, some of the liquid is also transferred onto the bare particle. This has been alluded to as the contact spreading mechanism in literature (Kontziampasis et al., 2020; Yusof et al., 2019).

Using image analysis, the change in red colour distribution throughout the dye spray-on process can be tracked as shown in Fig. 3(b). As the powder transitions from white to red in colour, the colour distributions shift towards the right (from ~greater % of red colour within the image) and become increasingly broader, whilst the maximum frequency value decreases. The variation in the maximum frequency value can be used as a tool to determine if the continuous coating process can achieve a steady state. To make the understanding of this analysis easier, the maximum frequency value of the uncoated powder is set as the reference value, which in this case is 1.8. The maximum frequency value obtained from each image is then subtracted from this reference value and plotted as shown in Fig. 3(c). Between $t = 0$ s and 18 s there is no change in the appearance of the powder (as can be seen visually in Fig. 3(a)) so the change in red is calculated as ~0 (i.e. the maximum frequency values obtained are very similar to the reference value). This is expected because the spray nozzle was turned on after 18 s in order to check if there was fluctuation in the red colour distribution of the white powder when measured continuously. From 27 s to around 45 s the change in colour intensity results in a decrease in the maximum frequency value obtained with time coinciding with a steep increase in Fig. 3(c). Above this period a plateau is observed indicating little or no change in the red colour intensity of the coated powder, thus indicating that the continuous spray-on method achieves a steady state.

Positron Emission Particle Tracking: Characterisation of the powder flow within the TSM was conducted by Positron Emission Particle Traking (PEPT), a radiation imaging technique developed at the University of Birmingham, UK (Parker et al., 1993). It is capable of tracking the three-dimensional trajectory of particles within the interior of a dense, opaque system with sub-mm spatial resolution and a temporal resolution on the millisecond scale. This capability allows us to study the powder behaviour within a TSM, which is not possible using other conventional imaging techniques. More detailed information and examples of the technique can be found elsewhere (Jones et al., 2007; Leadbeater et al., 2012; Mihailova et al., 2015; Parker et al., 1997).

To perform PEPT experiments, radioactive tracer particles that were similar in size and density to the sodium sulphate powder (to achieve similar flow patterns within the mixer) were prepared using a resin ion-exchange method (Parker & Fan, 2008). These tracer particles were labelled with a with a β^+-emitting

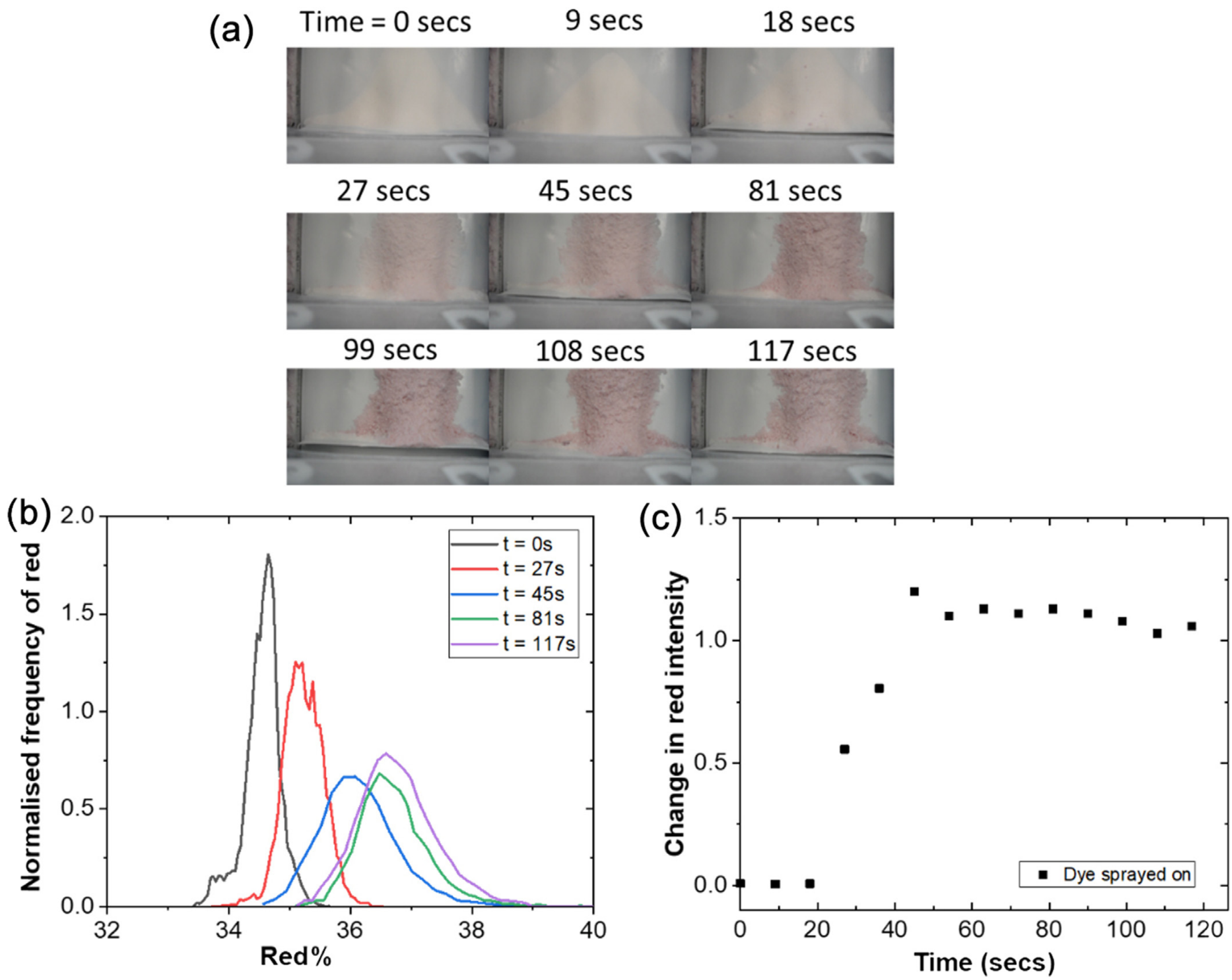

Fig. 3. (a) Images of spray coated sodium sulphate powder with the low viscosity red dye showing changes in red colour intensity with time, (b) the corresponding averaged normalised histograms of the red colour distribution within these powders and (c) tracking the difference in the peak value of the colour distributions of the coated powders vs. uncoated powder with processing time showing equilibrium (steady state) is achieved around 45 s. (For interpretation of the references to colour in this figure legend, the reader is referred to the Web version of this article.)

radioisotope, Fluorine-18, causing the emission of two high-energy gamma photons possessing opposite trajectories. The PEPT camera (two parallel plates of solid scintillating crystals of sodium iodide) detect and locate the gamma radiation (linear trajectories) from the decaying isotope allowing for instantaneous particle triangulation. These plates are 500 $\times$ 400 mm^2; which meant that the TSM 75, with a total axial length of 750 mm, could not fit completely within imaging zone. As a result only the last quarter of the axial length, from 450 to 615 mm, could be accurately recorded.

At the start of the experiment, the tracer particles were added into the TSM (via the top inlet port) one at a time into the moving powder bed. Upon exiting the TSM, this powder (containing the tracers) were collected and reintroduced into the powder hopper that fed the TSM until a total of 100 particle passes were acquired. The data acquired (cartesian coordinates and time) were analysed using MATLAB® to project the particle trajectories within a three-dimensional space. The data was smoothed to remove noise by applying a median filter (taking the median average over every five points) and any erroneous locations (due to scattering of gamma rays) were ignored.

3. Results and discussion

3.1. Effect of material parameters

To probe the process of wet coating of particles continuously using viscous liquids and their foam counterparts, several material parameters were examined. These were the following: 1) the effect of using viscous liquids vs. corresponding foams consisting of large (cm) sized bubbles, (small sized bubbles were not considered as part of this study due to poor coating performance in batch trials), 2) the effect of initial liquid viscosity on the resulting foams as a coating vehicle. The coating performance was evaluated by examining the colour distribution within the bulk powder, and additionally, the ability for the coating process to reach equilibrium. The powder feed rate and mixer motor speed were kept constant at 196 kg/h and 30 Hz, respectively.

Fig. 4(a) shows the calculated average histograms of red distribution of the powder coating process, when using: a) a viscous liquid (based on formulation 2), b) a big bubble foam (fabricated using this same liquid), and c) for comparison reasons the base dye solution only (very low viscosity liquid). It is evident that greater control in the colour distribution within the bulk powder is achieved when a big bubble foam is used in comparison to both the viscous liquid as well as the dye solution. The resultant average peak yields a narrower distribution and has a sharper taller peak, evidencing improved colour distribution. A hypothesis for this result is the following mechanism of coating. The big bubble foam occupies a large surface contact area (low localised liquid to solid ratio) when it falls onto the fluidised powder bed zone of the TSM mixer. The fluidisation of the powder causes the foam to ‘bump’ or float on top of the powder bed (Litster & Ennis, 2004), leading to additional deformation and elongation, which in turn increases the surface contact area even further. This deformation and elongation is most likely allowed in the case of foam, due to the low elastic shear modulus that is also documented in detergent foams (Weaire & Hutzler, 2001). The foam eventually gets pulled within the powder bed where it is mechanically dispersed by the quadrant paddles. During this stage, an interaction between the thin liquid films (that the foam is made of), the wetted, and the non-wetted particles will occur via the contact spreading mechanism. This will lead to a homogeneous colour distribution within the powder bed.

In contrast, when a liquid is poured onto the moving powder bed it only occupies a small surface contact area and produces a narrow band of wetted powder close to the contact zone. This localised contact surface area allows for the large liquid droplets to penetrate the powder bed, the rate of which is dependent on the liquid’s viscosity and the void fraction within the fluidised bed (Tan & Hapgood, 2011b). It should be noted that during this stage these liquid droplets act as a binder, connecting numerous primary particles together. Upon contact with the rotating blades these liquid bound particles are broken down into large granular materials that are dispersed both axially and radially. If the shear created by the paddles is able to overcome the strength of bound material during its residence time in the mixer, then it will disintegrate into non granular ‘crumb’ like particles. Upon contact with non-wetted particles liquid will transfer and lead to improvements in the overall colour distribution within the powder bed. This most likely occurs when the base dye solution is used, due to slight broadening of the distribution and a measured decrease in the height of its peak in combination with a small shift in the curve towards the right. In the case of the more viscous liquid, the colour distribution is much broader with a lower peak. This can be attributed to the inability of the blades to break up the agglomerates, leading to granules of dense, “concentrated” red in colour, compared to the bulk, and thus is observed as poor colour distribution and inhomogeneity within the bulk product. It should also be noted that if the viscous liquid comes into direct contact with the paddles during the coating process, it provides a site for powder makeup with variations in colour. The design of the paddles aims to reduce powder makeup and will additionally result in large agglomerates being released within the bulk influencing also the colour distribution. These mechanisms relating the interaction between an agitated powder bed in a twin screw mixer with the coating fluid via either i) the spray on of a low viscosity liquid, or ii) addition of a large bubble foam or iii) pouring of a viscous liquid are summarised in Fig. 5.

Tracking of the continuous coating process by evaluating changes in the maximum frequency value is presented in Fig. 4(b). The data shows that irrespective of the coating fluid used, the bulk powder transitions from an uncoated regime to a coated one (identified by plateau in the data). This transition period occurs much faster when using the low viscosity (1.13×10^{-3} Pa s) dye (between 10 and 20 s), compared to the use of the big bubble foam from a high viscosity liquid. The big bubble foam viscosity is difficult to measure but is expected to be lower than the base liquid viscosity of 0.17 Pa s that is associated to formulation 2, which was used as the default formulation in a previous study (Kontziampasis et al., 2020), whereas it is also the default formulation that is used in this study, unless stated otherwise (~40 s). The low viscosity of the base dye solution results in faster powder penetration times and is easily dispersed within the bulk powder mechanically. Once equilibrium is reached there is also less scatter in the data indicating that a steady state process is achieved. Increasing the viscosity of liquid (F2 liquid) results in the formation of granules that are concentrated in colour. These granules result in greater inhomogeneity in the bulk powder colour distribution leading to an increased scatter in the data once equilibrium in the coating/granulation process is achieved. We can hypothesise that this

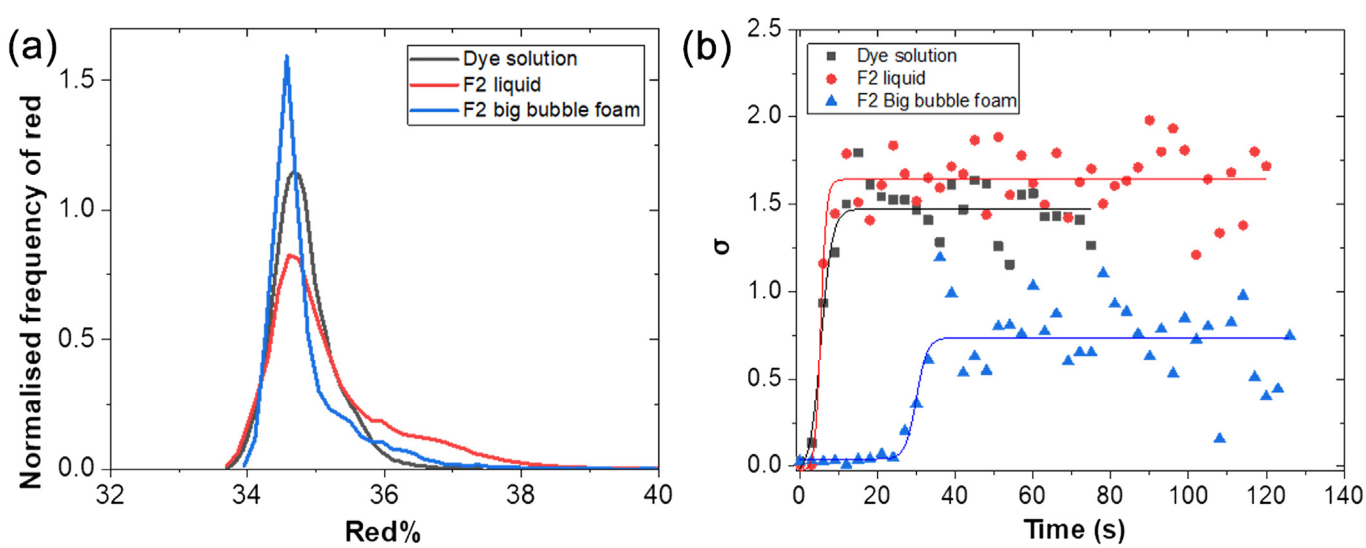

Fig. 4. (a) Averaged normalised histograms of red colour distribution for powders coated with a sprayed on dye, viscous liquid (formulation 2), and a big bubble foam prepared from formulation 2. The highest peak occurs in the case of big bubble foam and the broadest peak in the case of the viscous liquid and (b) change in red colour intensity compared to base powder with processing time using the sprayed on dye, viscous liquid, and the corresponding big bubble foam. (For interpretation of the references to colour in this figure legend, the reader is referred to the Web version of this article.)

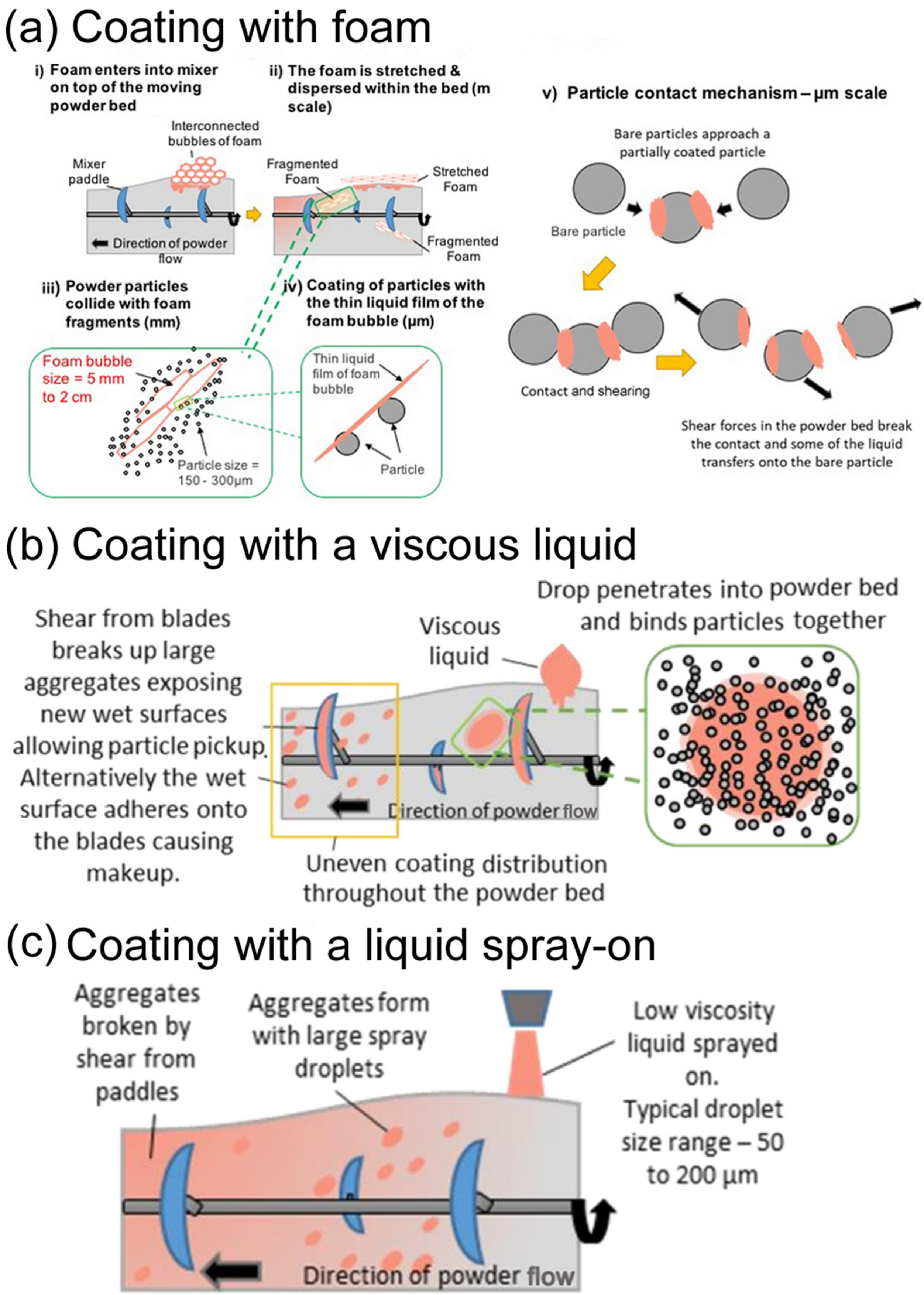

Fig. 5. Illustration of the mechanisms at play when coating an agitated powder bed using (a) large bubble foam, (b) pouring on a high viscosity liquid and (c) spray-on of a low viscosity fluid.

occurs due to the high viscosity, since the formulation needs a longer time to penetrate and disperse within the powder bed as alluded to by Hapgood et al. (Hapgood et al., 2002). This results in high localised liquid concentrations, subsequently leading to agglomeration. The broadness in the frequency distribution curves and a low maximum frequency value of the liquid dye and liquid formulation (when compared to the base powder) leads to the plateau values occurring around 1.5. In comparison, the big bubble foam takes longer to penetrate into the powder bed (i.e. a longer residence time in the mixer) so the time taken for the transition from uncoated to coated is much higher. The plateau value occurs around 0.7 indicating less variance in the red colour distribution compared to the base powder. This is because when coating with foams continuously, the overall thin liquid film to solid ratio is much lower than that occurring when using liquids. As a result, the intensity of the coating applied is low, and we observe a reduced tendency for agglomeration. This thin coating means that that there is less tendency for the particle to agglomerate and the base powder colour properties still play a dominant role in the subsequent colour analysis. We attribute the scatter in data around the plateau to the periodicity of the foam entering the mixer i.e. pulsing as evident in the video of the supplementary data.

The effect of the starting liquid viscosity on the coating performance when converted to big bubble foams is presented in Fig. 6. Examining the average red colour distribution curves as a function of initial liquid viscosity shows minor variations with increasing viscosity (Fig. 6(a)). Using big bubble foams produced with a F1 liquid yields a narrow distribution with a sharp peak indicating homogenous coating of the bulk powder. As the viscosity is increased, the distributions shift slightly to the left indicating a decrease in the % of red within the sample. The distributions also become broader and the maximum frequency peak height reduces as a result. Although the rheological properties of these foams have not been characterised, we expect that the liquid viscosity (Newtonian in behaviour (Kontziampasis et al., 2020)) is retained for the liquid films connecting air bubbles. However, the overall viscosity of the bulk foam will be lower than that of the initial liquid. As a consequence, with increasing viscosity the deformation and elongation process of the foam will take longer, implying a longer residence time within the powder bed is required. Since the powder is conveyed forward continuously, this equates to a lower contact time with powder and may explain the broadness in the colour distribution. When assessing the coating performance continuously (Fig. 6(b)) it was found that F1, F2 and F3 performed similarly achieving a plateau value after 18 s. In the case of F4, a large amount of data scatter can be seen indicating a high level of variability in the colour distribution of the bulk powder. This supporting the hypothesis of a short foam-to-powder contact time leading to inhomogeneity.

3.2. Effect of process parameters

In addition to studying the effect of formulation properties, there is also a need to understand the effect of processing parameters on the coating distribution. In this study, the influence of the following factors was considered: i) effect of mixer motor speed and ii) powder fill level (altering the foam to powder ratio). Foams with big bubbles created from Formulation 2 were used as the default coating formulation.

The influence of mixer speed on the average powder red colour distribution and the transition from uncoated to coated material is presented in Fig. 7.

The mixer motor speed controls the shear forces that the quadrant paddles impart on the bulk powder bed and big bubble foam. The best quality of coating (in terms of colour distribution) is achieved when the TSM operates at 30 Hz as evident by narrowest colour distribution and the sharpest peak (Fig. 7(a)). This matches well with observations conducted during batch processing in our previous study (Kontziampasis et al., 2020). Additionally, there is limited scatter in data as the powder transitions from uncoated to coated (Fig. 7(b)). Operating at 15 Hz, the red colour distribution broadens with a bi-modal distribution and there is a large reduction in the maximum frequency value (lowest out of the 3 speeds studied) obtained. In addition, the peak position shifts towards the right indicating that the red % detected in the bulk powder is higher. This suggests that at this speed the mixer generates shear forces that allows the foam to elongate and deform, but is not sufficient to break and mechanically disperse within the powder bed. This lends itself to the formation of highly concentrated colour regions within the bulk powder, giving rise to both colour inhomogeneity and a shift in the red colour observed. Increasing the speed to 70 Hz, leads to the broadest distribution and the peak shift towards the left indicating a low % of red colour within the bulk powder. At this speed the foam undergoes rapid deformation and is easily broken by the paddles. However, the paddles also convey the powder much faster meaning a higher throughput and lower foam residence time. This corresponds to a faster transition time (Fig. 7(b)) and a large amount of scatter in the data, which explains the broadness and the low level of coating achieved.

In contrast to the batch studies (Kontziampasis et al., 2020), increasing the powder fill level within the mixer (by increasing the screw feeder/hopper throughput from 5 Hz to 9 Hz, i.e. 196 and 405 kg/h) leads to a slight broadening of the average distribution and a reduction in the peak value of the maximum frequency (Fig. 8(a)). This change was found to be significant when performing a simple *t*-test with a p-value $= 0.05$. These studies were conducted at a fixed mixer motor speed of 30 Hz. A shoulder in the colour distribution is also observed at lower % of red values, indicating less coating material is detected within the powder bed (large variation between the two fill levels as shown in Fig. 8(b)). This can be explained by a low foam to powder ratio as the foam addition rate remains unchanged whilst the powder throughput is doubled. It should be noted that by simply increasing the foam addition rate does not guarantee a match in coating performance. This is because the higher powder fill level will result in the foam ‘bumping’ on the powder surface for longer upon contact before being roped into the bulk powder. An example of the foam being stretched and bumping on the powder bed can be seen in Video S1 as part of the supplementary data.

3.3. Mixer scale-up considerations

To understand the implication of mixer size on the coating process a comparative study between the TSM 75 and a TSM 125 was conducted. The overall red colour distribution within the bulk powder throughout the coating process was compared using formulation 2, both as a liquid (poured on) and as a big bubble foam (Fig. 9(a)). In the case of the TSM 75 the big bubble foam produces a sharp peak and a narrow distribution, whereas the poured-on liquid produced a broad distribution with a shallow peak. In contrast, when using the TSM 125 there was no observable difference in the distribution between the liquid and foam. Both red colour distributions are broad and the peak values are much lower than those obtained with the TSM 75. Also, the relative peak positions are shifted to the left around 34 red % which is similar to the peak position of the base uncoated powder. The broadness of the distribution and low peak value indicates that the coating material is being applied onto the base powder. However, the colour change is very subtle with the underlying base powder colour properties still remaining dominant due to the peak position obtained. This

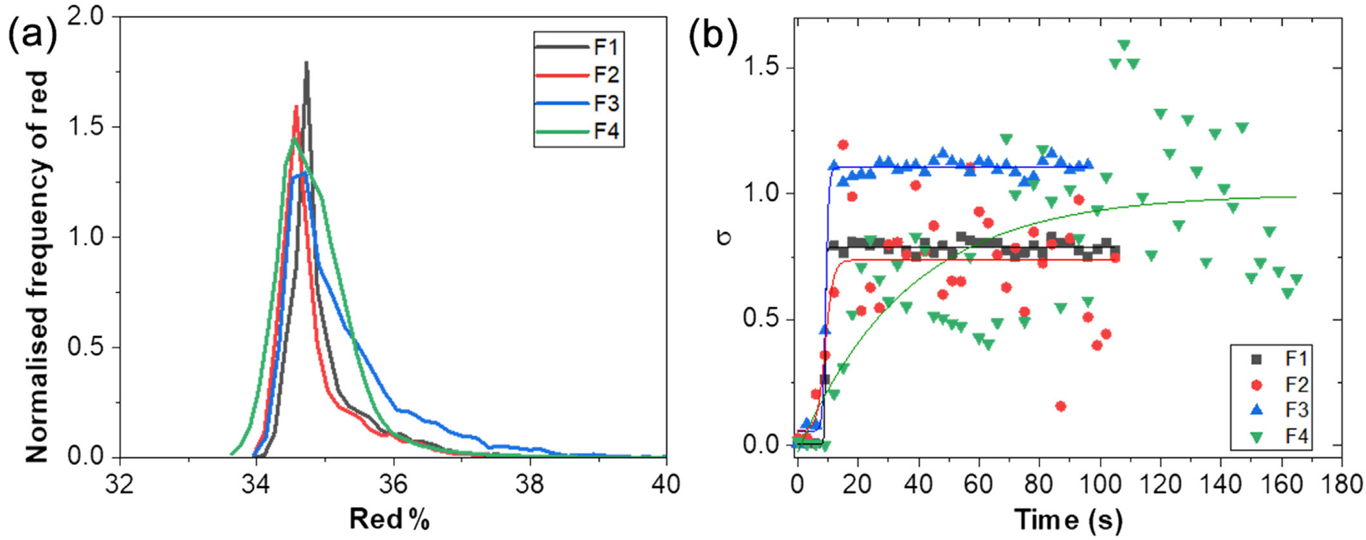

Fig. 6. (a) Averaged normalised histograms of red colour distribution for powders coated with big bubble foams from liquids with increasing viscosity and (b) change in red colour intensity compared to base powder with processing time. (For interpretation of the references to colour in this figure legend, the reader is referred to the Web version of this article.)

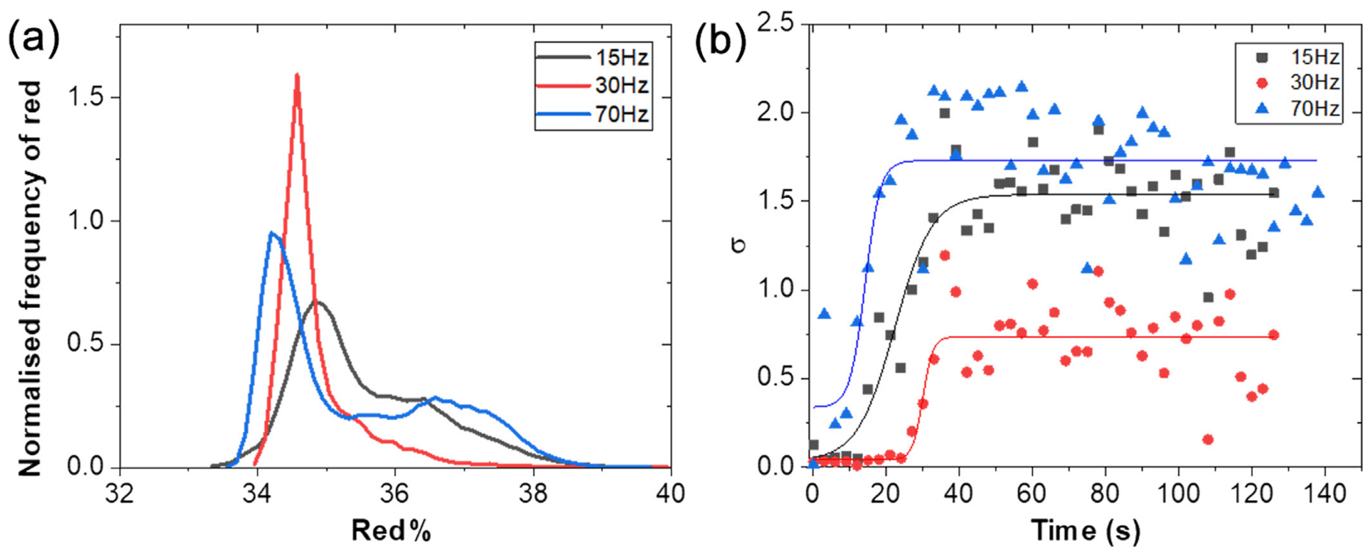

Fig. 7. (a) Average normalised histograms of red colour distributions for powders coated using big bubble foam (based on formulation 2) as a function of mixer motor speed and (b) variation in red colour intensity compared to base powder with processing time. (For interpretation of the references to colour in this figure legend, the reader is referred to the Web version of this article.)

can be explained when probing the process conditions further. To achieve the same powder fill level in the TSM 125, the powder feeder was operated at 9 Hz instead of 5 Hz. The coating fluid dosage rates were kept unchanged for both mixers and as a result the overall ratio of coating material vs. powder was lower in the larger mixer.

The effect of mixer motor speed also showed the same trend (Fig. 9(b)) when using big bubble foam as the coating media (based on formulation 1.5). Although the mixer motor speeds selected were the same, the effective tip speeds achieved with the TSM 125 are lower due to the larger mixer size. For example, at a motor speed of 30 Hz the TSM 125 produces a tip speed of 0.31 m/s compared to 0.5 m/s with the TSM 75. Based on these results, exploring different coating fluid dosing levels and mixer tip speeds would have provided further insight into how scalable the mixers are. Unfortunately, due to limitations in the experimental time at the pilot scale facility this was not feasible.

During these mixer comparison studies it was found that when agglomeration occurred instead of coating, there was a noticeable difference in how the bulk powder exited the mixers onto the conveyor belt. This is illustrated in the digital micrographs presented in Fig. 10 for both mixers. It can be seen that in the case of TSM 75, the agglomerates produced appear to accumulate more on the left hand side whereas they appear more evenly distributed when using the TSM 125. This was also seen when the TSM 75 mixer was loaded with coloured particles to assess how well they distributed within the bulk powder. The resulting images showing this skew can be found in Fig. S2 in the supplementary data. This bias can also be visualised when performing image analysis of the bulk powder both continuously and as an overall distribution, which does not occur in the case of TSM 125. This indicates that

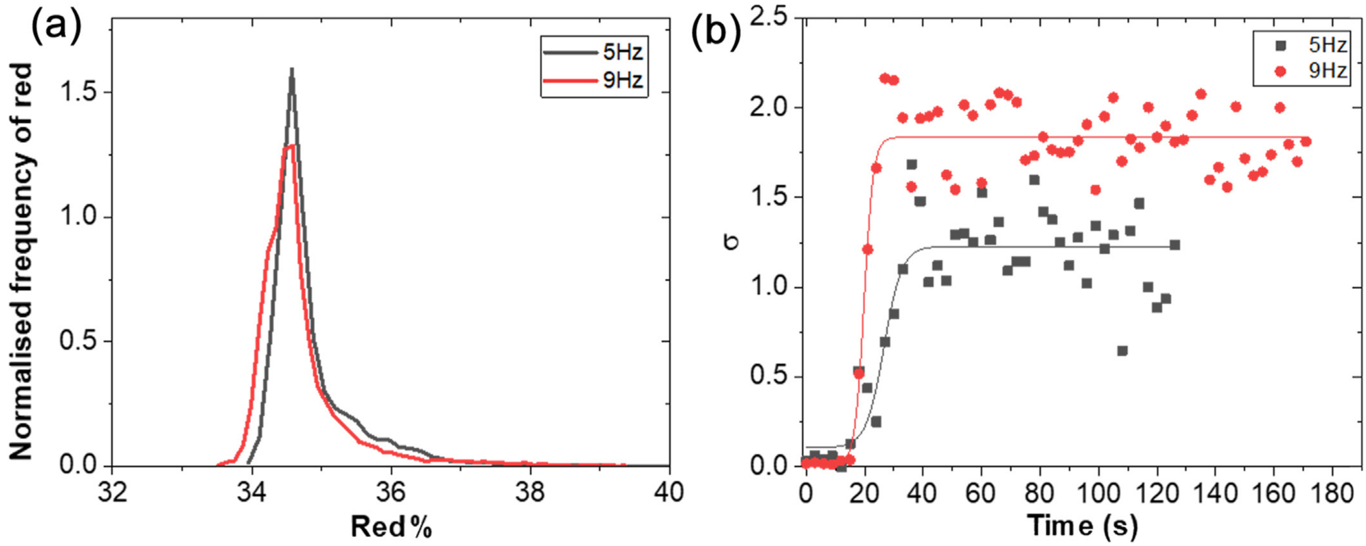

Fig. 8. (a) Average normalised histograms of red colour distributions for powders coated using big bubble foam (based on formulation 2) as a function of powder hopper feed rate (controlling the powder fill level in the TSM) and (b) variation in red colour intensity compared to base powder with processing time. (For interpretation of the references to colour in this figure legend, the reader is referred to the Web version of this article.)

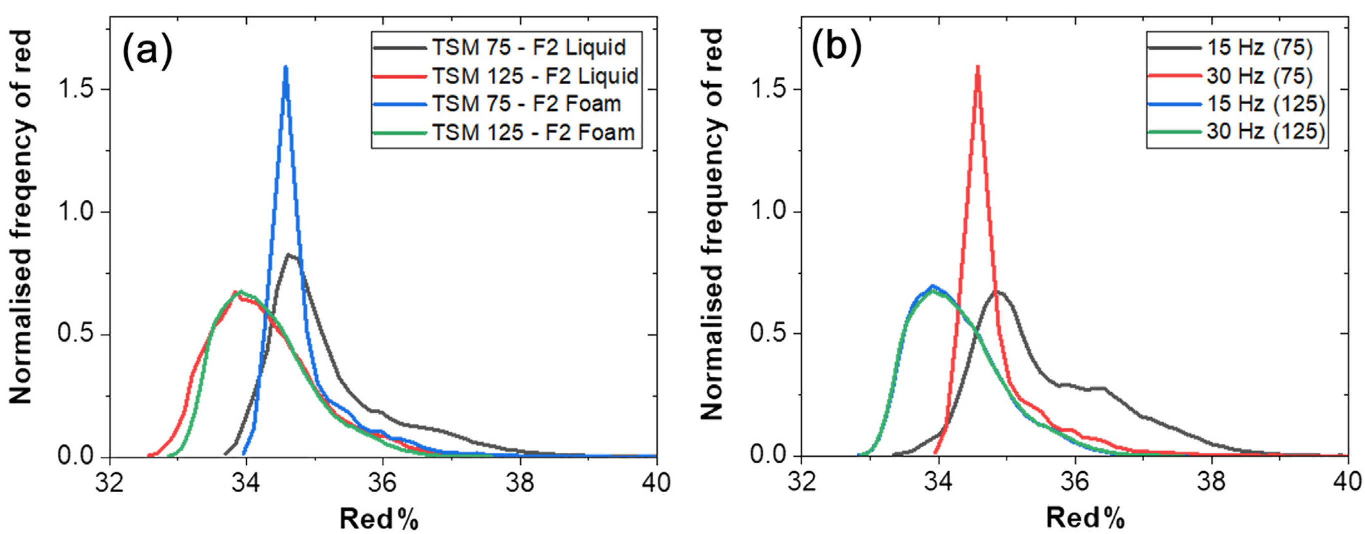

Fig. 9. Average normalised histograms of red colour distributions for powders coated using the TSM 75 and 125 mixers illustrating (a) performance of liquid vs foam (based on Formulation 2) and (b) effect of mixer motor speed. (For interpretation of the references to colour in this figure legend, the reader is referred to the Web version of this article.)

there is a preference for these granules to reside within the left hand screw of the TSM.

Positron Emission Particle Tracking (PEPT) is a useful tool to understand the characteristics of the mixer by tracking the mixer occupancy and paths taken by the radioactive tracer particles. A plot of particle occupancy within the TSM 75 mixer is presented in Fig. 11(a). It can be seen that on average the particles reside close to the right shaft at the mixer entrance region and then shift towards the left shaft prior to exiting the mixer. Furthermore, the tracking of 3 randomly selected particle paths (out of a 100 paths) also support the notion of this shaft preference (Fig. 11(b)). It is not known what causes this to occur, it could be down to the screw, paddle setup or improper balance, however it does highlight the challenges associated with understanding the scalability of the process.

For future industrial coating applications using the TSM, there is a need to understand the mechanism of coating when foams are used especially relating the rheological behaviour (based on bubble size) to coating performance. The challenge here is to characterise the rheological properties of the larger bubble-based foams. This information is particularly important for foams based on very viscous fluids as experimental data shows that they require longer residence times in the mixer to fully break down and coat the particles. A solution to this is to increase the mixer axial length or to have numerous TSM's operating in series. For scaling up the coating operation there are a number of parameters that would need to be kept constant; i) the mixer tip speed (instead of using the motor speed) or similar Froude numbers, ii) the coating fluid to powder ratio based on the desired product throughput (although there will be a limit as to how much can be added before agglomeration dominates if no drying steps are in place), and iii) the powder fill height. In addition, a check on the mixer screw alignment should be done (experimental and PEPT data highlights the importance of this) to ensure that the product has a homogenous distribution upon exit from the mixer.

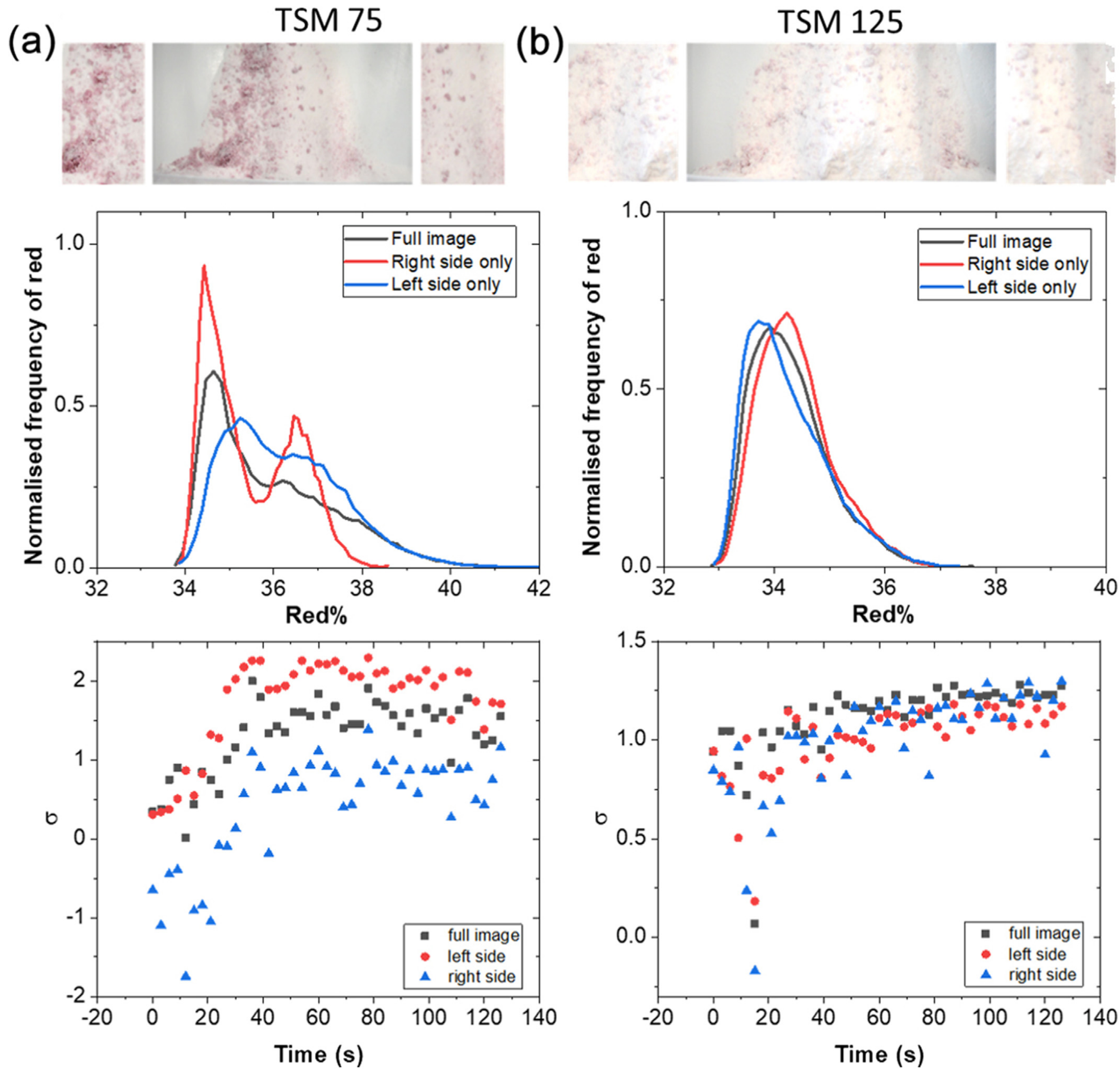

Fig. 10. Comparing image analysis of a full image vs the left/right hand side contributions on the average normalised red colour histograms and change in red intensity with respect to the base powder as a function of processing time when using (a) TSM 75 and (b) 125. (For interpretation of the references to colour in this figure legend, the reader is referred to the Web version of this article.)

4. Conclusions

In this study we evaluate the use of a twin screw mixer operating continuously to determine the effectiveness of foams and liquids as a means for coating powder beds. It is shown that the use of large bubble foams (based on high viscosity liquids) leads to a better powder coating performance compared to the viscous liquid counterparts. This is realised by the better dispersion of the additive in the agitated powder bed and less tendency of the particles to aggregate.

Scale up of the mixers is a non-trivial exercise and the results indicate that that a number of different factors will influence this, including shaft speed, powder fill levels, residence time and diameter of the shafts. Additionally, this imbalance between the two shafts can result in a bias causing the product to favour along one side vs. the other as sorted by the PEPT data. It should be noted that as with any liquid coating operation there is a limit to the amount of liquid added before the system will start to agglomerate if there are no intermediate drying steps involved. However, the ability to convert concentrated, viscous liquids to foams as coating

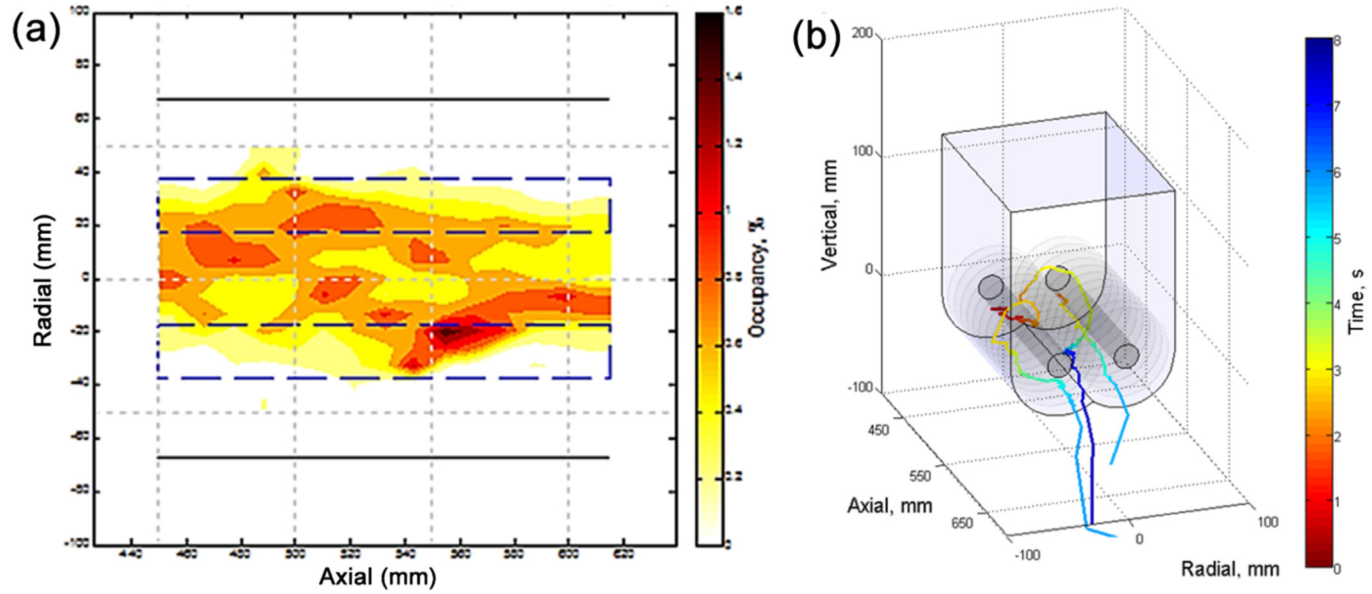

Fig. 11. Illustration of (a) a top-down particle occupancy plot comparing the radial and axial mixing (with a high occupancy towards one shaft prior to particle exit) and (b) 3 random particle trajectories (taken from 100 passes) from analysis of Positron Emission Particle Tracking data.

agents allows more active addition vs diluting the liquid for atomisation.

CRediT authorship contribution statement

Mohamed S. Manga: Writing – review & editing, Writing – original draft, Visualization, Validation, Methodology, Investigation, Formal analysis, Conceptualization. **Dimitrios Kontziampasis:** Writing – review & editing, Visualization, Validation, Software, Project administration, Methodology, Investigation, Formal analysis, Conceptualization, Resources. **Mustafa Al-Maqdad:** Formal analysis, Data curation. **Sean Clifford:** Methodology, Formal analysis, Data curation. **Serafim Bakalis:** Writing – review & editing, Resources, Conceptualization. **David W. York:** Writing – review & editing, Supervision, Resources, Project administration, Funding acquisition, Conceptualization.

Declaration of competing interest

The authors declare that they have no known competing financial interests or personal relationships that could have appeared to influence the work reported in this paper.

Acknowledgements

This work is funded by Innovate UK, AMSCI and BIS (Grant number: 31587-233189) as part of the Chariot project. The authors would like to thank Mr. Robert Harris for his help in the fabrication of the continuous foaming machine used in this study as well as his help in various technical matters of this work. The authors acknowledge the contribution of Mr. Thomas Coyle and Mr. Chester Aguirre in setting up and aiding with the continuous studies at the Centre of Process Innovation, Sedgefield, U.K. We also want to thank Procter and Gamble and AJAX Instruments Ltd for the fruitful discussions and support in providing some of the materials used in this study, as well as for technical discussions regarding the TSM. Finally, the authors would like to thank Dr. Olga Mihailova, Mr. Jerome Castro, Mr. Chris Bowman, Dr Dimitrios Karampalis, Ms Vasiliki Kafourou, and Ms Larisa Onoufriadi for their assistance during the PEPT TSM experiments, as well as to Dr. Thomas Leadbeater for preparing the radioactive tracers.

Appendix A. Supplementary data

Supplementary data to this article can be found online at https://doi.org/10.1016/j.partic.2024.07.012.

References

Cantor, S. L., Kothari, S., & Koo, O. M. Y. (2009). Evaluation of the physical and mechanical properties of high drug load formulations: Wet granulation vs. novel foam granulation. *Powder Technology, 195*, 15–24.
Cole, G. (1995). Introduction and overview of pharmaceutical coating. *Pharmaceutical coating technology*. CRC Press.
Ennis, B. J. (2010). Agglomeration technology: Equipment selection. *Chemical Engineering, 117*, 50–54.
AJAX Equipment, Twin Screw Machines, Available at: https://www.ajax.co.uk/mixtheory.htm.
Fuchs, M., Turchiuli, C., Bohin, M., Cuvelier, M. E., Ordonnaud, C., Peyrat-Maillard, M. N., & Dumoulin, E. (2006). Encapsulation of oil in powder using spray drying and fluidised bed agglomeration. *Journal of Food Engineering, 75*, 27–35.
Gregorian, R. S., Bafford, R. A., & Namboodri, C. G. (1979). The utilization of foams in the wet processing of textiles, Energy Conservation in Textile and Polymer Processing. *American Chemical Society*, 155–173.
Hapgood, K. P., Litster, J. D., Biggs, S. R., & Howes, T. (2002). Drop penetration into porous powder beds. *Journal of Colloid and Interface Science, 253*, 353–366.
Hapgood, K. P., Litster, J. D., & Smith, R. (2003). Nucleation regime map for liquid bound granules. *AIChE Journal, 49*, 350–361.
Iveson, S. M., & Litster, J. D. (1998). Growth regime map for liquid-bound granules. *AIChE Journal, 44*, 1510–1518.
Iveson, S. M., Wauters, P. A. L., Forrest, S., Litster, J. D., Meesters, G. M. H., & Scarlett, B. (2001). Growth regime map for liquid-bound granules: Further development and experimental validation. *Powder Technology, 117*, 83–97.
Jones, J., Parker, D., & Bridgwater, J. (2007). Axial mixing in a ploughshare mixer. *Powder Technology, 178*, 73–86.
Keary, C. M., & Sheskey, P. J. (2004). Preliminary report of the discovery of a new pharmaceutical granulation process using foamed aqueous binders. *Drug Development and Industrial Pharmacy, 30*, 831–845.
Genttä, E., Kinnunen-Raudaskoski, K., & Hjelt, T. (2014). Characterization of thin pigment coating layers produced by foam coating. *Tappi Journal, 13*, 21–27.
Kinnunen-Raudaskosko, K., Hjelt, T., Kenttä, E., & Forsström, U. (2014). Thin coatings for paper by foam coating. *Tappi Journal, 13*, 9–19.
Kontziampasis, D., Manga, M. S., & York, D. W. (2020). Coating particles using liquids and foams based on viscous formulations with industrial mixers: Batch operation. *Particuology, 50*, 13–24.

Leadbeater, T. W., Parker, D. J., & Gargiuli, J. (2012). Positron imaging systems for studying particulate, granular and multiphase flows. *Particuology, 10*, 146–153.

Li, H., Thompson, M. R., & O'Donnell, K. P. (2015). Progression of wet granulation in a twin screw extruder comparing two binder delivery methods. *AIChE Journal, 61*, 780–791.

Li, H., Thompson, M. R., & O'Donnell, K. P. (2015). Examining drug hydrophobicity in continuous wet granulation within a twin screw extruder. *International Journal of Pharmaceutics, 496*, 3–11.

Litster, J., & Ennis, B. (2004). *The science and engineering of granulation processes*. New York: Springer Science & Business Media.

Mihailova, O., Lim, V., McCarthy, M. J., McCarthy, K. L., & Bakalis, S. (2015). Laminar mixing in a SMX static mixer evaluated by positron emission particle tracking (PEPT) and magnetic resonance imaging (MRI). *Chemical Engineering Science, 137*, 1014–1023.

Nedovic, V., Kalusevic, A., Manojlovic, V., Levic, S., & Bugarski, B. (2011). An overview of encapsulation technologies for food applications. *Procedia Food Science, 1*, 1806–1815.

Onwulata, C. (2005). *Encapsulated and powdered foods*. CRC Press.

Parker, D., Broadbent, C., Fowles, P., Hawkesworth, M., McNeil, P. J. N. I., & S. (1993). Methods in physics research section A: Accelerators, detectors, A. Equipment. *Positron emission particle tracking-a technique for studying flow within engineering equipment, 326*, 592–607.

Parker, D., Dijkstra, A., Martin, T., & Seville, J. (1997). Positron emission particle tracking studies of spherical particle motion in rotating drums. *Chemical Engineering Science, 52*, 2011–2022.

Parker, D. J., & Fan, X. J. P. (2008). *Positron emission particle tracking—Application and labelling techniques, 6*, 16–23.

Paul, E. L., Atiemo-Obeng, V. A., & Kresta, S. M. (2004). *Handbook of industrial mixing: Science and practice*. New Jersey: John Wiley & Sons.

Plank, R., Diehl, B., Grinstead, H., & Zega, J. (2003). Quantifying liquid coverage and powder flux in high-shear granulators. *Powder Technology, 134*, 223–234.

Rocca, K. E., Weatherley, S., Sheskey, P. J., & Thompson, M. R. (2015). Influence of filler selection on twin screw foam granulation. *Drug Development and Industrial Pharmacy, 41*, 35–42.

Rough, S. L., Wilson, D. I., & York, D. W. (2005). A regime map for stages in high shear mixer agglomeration using ultra-high viscosity binders. *Advanced Powder Technology, 16*, 373–386.

Salman, A. D., Hounslow, M., & Seville, J. P. (2007). *Handbook of powder technology, granulation*. Amsterdam: Elsevier.

Sheskey, P., Keary, C., Clark, D., & Balwinski, K. (2007). Scale-up trials of foam-granulation technology - high shear. *Pharmaceutical Technology, 31*, 94–108.

Sievänen, H. (2010). *Suitability of foam coating on application of thin liquid films*. Masters' Thesis. Lappeenranta University of Technology.

Tan, M. X. L., & Hapgood, K. P. (2011a). Foam granulation: Liquid penetration or mechanical dispersion? *Chemical Engineering Science, 66*, 5204–5211.

Tan, M. X. L., & Hapgood, K. P. (2011b). Foam granulation: Binder dispersion and nucleation in mixer-granulators. *Chemical Engineering Research and Design, 89*, 526–536.

Tan, M. X. L., Wong, L. S., Lum, K. H., & Hapgood, K. P. (2009). Foam and drop penetration kinetics into loosely packed powder beds. *Chemical Engineering Science, 64*, 2826–2836.

Thompson, M. R. (2015). Twin screw granulation – review of current progress. *Drug Development and Industrial Pharmacy, 41*, 1223–1231.

Thompson, M. R., Mu, B., & Sheskey, P. J. (2012). Aspects of foam stability influencing foam granulation in a twin screw extruder. *Powder Technology, 228*, 339–348.

Thompson, M. R., & O Donnell, K. P. (2015). "Rolling" phenomenon in twin screw granulation with controlled-release excipients. *Drug Development and Industrial Pharmacy, 41*, 482–492.

Thompson, M. R., Weatherley, S., Pukadyil, R. N., & Sheskey, P. J. (2012). Foam granulation: New developments in pharmaceutical solid oral dosage forms using twin screw extrusion machinery. *Drug Development and Industrial Pharmacy, 38*, 771–784.

Weaire, D. L., & Hutzler, S. (2001). *The physics of foams*. Oxford University Press.

Weatherley, S., Thompson, M. R., & Sheskey, P. J. (2013). A study of foam granulation and wet granulation in a twin screw extruder. *Canadian Journal of Chemical Engineering, 91*, 725–730.

Wurster, D. E. (1959). Air-suspension technique of coating drug particles - a preliminary report. *Journal of the American Pharmaceutical Association, 48*, 451–454.

Yusof, N., Green, J., Pitt, K., Arjmandi-Tash, O., Campbell, A. I., Ahmadian, H., Tantawy, H., & Smith, R. (2019). A novel method for the analysis of particle coating behaviour via contact spreading in a tumbling drum: Effect of coating liquid viscosity. *Powder Technology, 351*, 102–114.